Materials Letters 191 (2017) 69–72

Contents lists available at ScienceDirect

Materials Letters

journal homepage: www.elsevier.com/locate/mlblue

Influence of post-calcination grinding on the properties of $Ba_{0.85}Ca_{0.15}Zr_{0.1}Ti_{0.9}O_3$ lead-free piezoceramics

A. Di Loreto [a,b], A. Frattini [a,b], M.G. Stachiotti [a,*]

[a] Instituto de Física Rosario, Universidad Nacional de Rosario-CONICET, 27 de Febrero 210 Bis, 2000 Rosario, Argentina
[b] Área Física, Dpto. de Química Física, FCByF, Universidad Nacional de Rosario, Argentina

ARTICLE INFO

Article history:
Received 15 July 2016
Received in revised form 2 January 2017
Accepted 7 January 2017
Available online 9 January 2017

Keywords:
Ferroelectrics
Lead-free piezoelectrics
BCZT ceramics

ABSTRACT

The effects of the post-calcination grinding on the structural and electrical properties of $Ba_{0.85}Ca_{0.15}Zr_{0.1}Ti_{0.9}O_3$ (BCZT) lead-free ceramics were investigated. We show that an intense degree of milling affects drastically the structural homogeneity and deteriorates the electrical properties of the ceramics. This occurs due to a phase decomposition process mechanically activated by the grinding. The resulting microstructure consists of BCZT grains, $CaTiO_3$ nanocubes and an amorphous phase rich in Ba and Ti.

1. Introduction

The dominant materials for practical application of piezoelectric devices are lead-based systems, such as $PbZr_xTi_{1-x}O_3$ (PZT) because of their superior ferroelectric and piezoelectric properties. Due to the high toxicity of lead, there is an increasing interest in developing alternative piezoelectric materials, which are lead-free, environmental friendly and biocompatible [1–6]. $Ba_{0.85}Ca_{0.15}Zr_{0.1}Ti_{0.9}O_3$ (abbreviated as BCZT) is regarded as one of the most promising, because of its excellent dielectric, piezoelectric and ferroelectric properties [7–10]. This material displays an outstanding d_{33} piezoelectric coefficient, which is noticeably higher than that of other lead-free piezoelectric ceramics.

The most used technique to fabricate BCZT ceramics is the solid-state reaction route (SSR). However, the electrical properties of BCZT ceramics fabricated by SSR are difficult to reproduce. For instance, samples prepared by this technique have shown noticeable differences in the position and width of the ferroelectric peak. While it is generally accepted that the tetragonal-cubic phase transition (T_C) occurs at ~95 °C, there is some dispersion in the temperature position of the ferroelectric peak, and T_C values as low as 65 °C [11] have been reported. The piezoelectric coefficients also display great dispersion: d_{33} values between 200 and 600 pC/N have been reported in the literature [7,9,11–13]. The dispersion of electrical properties mainly arises from the complex nature of the BCZT solid solutions. For instance, it is well known that a precise control of the stoichiometry of zirconium is necessary to obtain good properties: T_C, the remnant polarization and the d_{33} coefficient decrease as the Zr content increases from 10% [14]. Grain size also affects the piezoelectric properties, but without altering T_C [9]. In this work, we demonstrate that the post-calcination grinding is another key parameter for a proper sintering of BCZT piezoceramics. As far as we know, there are no other studies on this topic. We show here that an intense milling degree deteriorates the electrical properties of the ceramics due to the development of an inhomogeneous microstructure.

2. Experimental procedure

BCZT powder was synthesized from a mixture of $BaCO_3$, $CaCO_3$, ZrO_2 and TiO_2 using a planetary ball mill equipment (Torrey Hills Technologies ND 0.4 L). This powder was milled in a liquid medium with zirconium balls, dried and calcined at 1300 °C during 4 h. Then, the calcined powder was divided in half to carry out two different grindings: wet and dry milling conditions. The first one was performed employing 3 g of powder in 10 ml of alcohol. Both post-calcination grindings were made with zirconium balls (ball/powder weight ratio = 10) during 6 h. The obtained powders were mixed with a polyvinyl butyral (PVB) binder solution and then die-pressed into disks (Ø10 mm × 2 mm). The pellets were sintered at 1400 °C by 6 h.

Crystal structure was analyzed by X-ray diffraction (XRD) using a Philips X'Pert Pro X-ray diffractometer. The microstructure and composition was examined by SEM using a FEI Quanta 200 FESEM Environmental and EDAX detector. For electrical studies, silver

* Corresponding author.
E-mail address: stachiotti@ifir-conicet.gov.ar (M.G. Stachiotti).

http://dx.doi.org/10.1016/j.matlet.2017.01.034
0167-577X/

electrodes were sputtered on both sides of the samples. Dielectric properties were measured using an LCR meter (QuadTech 7600 plus) attached to a programmable furnace. The d_{33} coefficient was measured by a Berlincourt-type d_{33} meter (KCF technologies, model PM3001). The poling was performed at room temperature by applying a field of 2 kV/mm for 30 min.

3. Results and discussion

Fig. 1 shows X-ray patterns and SEM images of calcined powders with different grinding treatments: non-milled powder (NM), milled in liquid medium (LM), and milled in dry conditions (DM). All powders show perovskite structure with the presence of small amounts of secondary phases. The NM powder (Fig. 1b) displays an average particle size of 300 nm with the typical formation of sintering necks between particles. The powder milled in liquid medium displays a similar particle size but the necks were broken by the grinding (Fig. 1c). Fig. 1d shows that the milling in dry conditions reduces the particle sizes. Particles with dimensions smaller than 100 nm are observed. This refinement in particle size is also reflected in the broadening of the X-ray diffraction peaks.

Fig. 2 shows X-ray patterns of ceramics fabricated with LM and DM powders. The thermal treatment stabilizes a single perovskite phase in the LM sample (the secondary phases observed in the powder are not detected in the ceramic). The situation is different however for the DM sample where the impurity peaks, detected in the calcined powders, remain after the sintering process. These peaks at ~33°, 47.5°, and 59° are assigned to $CaTiO_3$. Even more, at low angles the pattern shows a small hunchback background indicating the presence of amorphous phase.

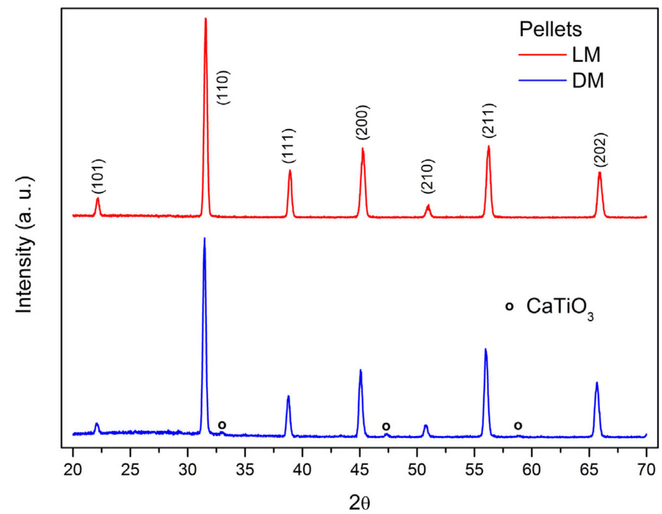

Fig. 2. XRD patterns of BCZT ceramics prepared with powders milled in liquid medium (LM), and milled in dry conditions (DM). The pellets were sintered at 1400 °C for 6 h.

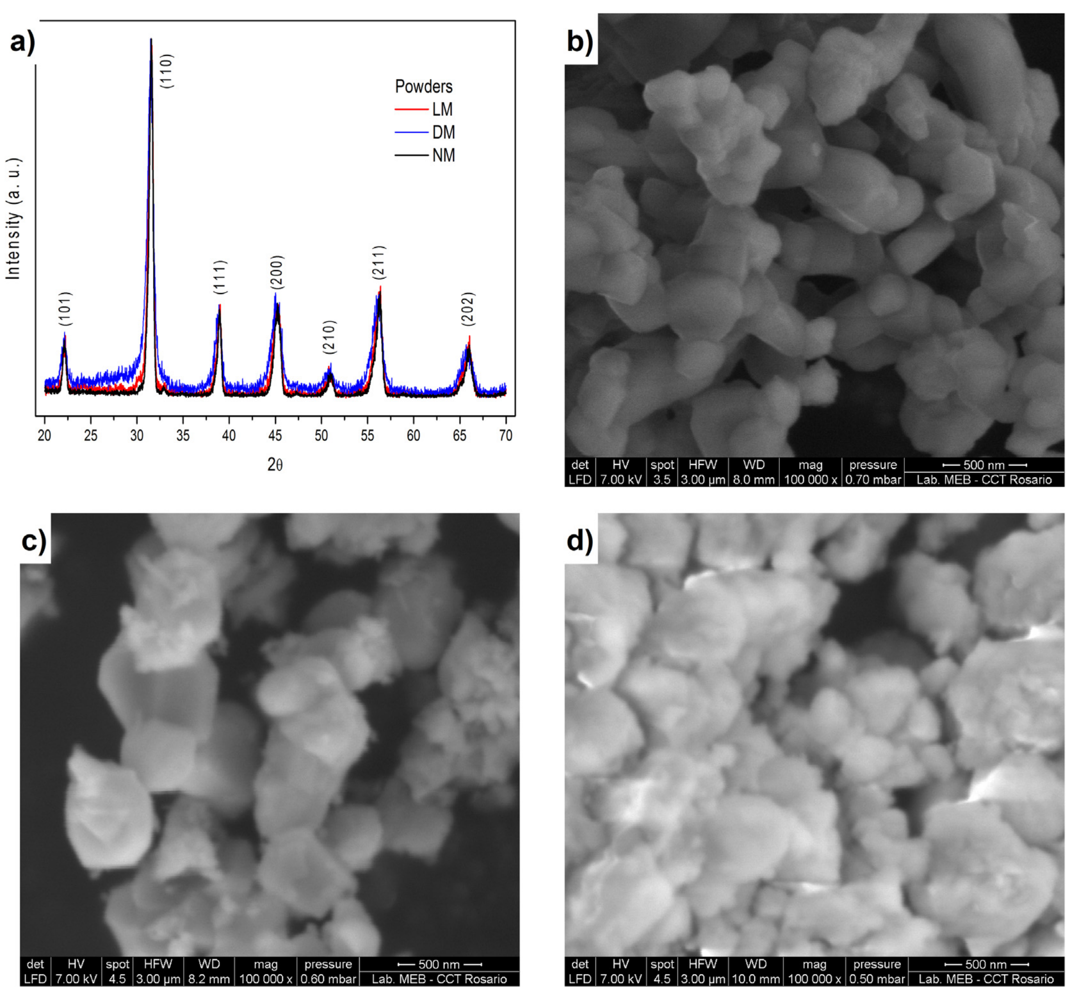

Fig. 1. (a) X-ray patterns of calcined powders with different grinding treatments: non-milled (NM), milled in liquid medium (LM), and milled in dry conditions (DM). SEM images of the BCZT powders: NM (b), LM (c) and DM (d).

Fig. 3a shows the temperature dependence of the dielectric constant for the LM and DM ceramics. The corresponding losses (not shown here) are all below 3%. It is clear that T_C depends on the grinding process of the calcined powders. While the LM sample displays a phase transition peak at ~96 °C, the DM sample shows a shift of the ferroelectric peak towards the low-temperature region (the maximum occurs at ~40 °C). The peak becomes wider and displays signatures of a relaxor-like behavior. Room-temperature polarization hysteresis curves are shown in Fig. 3b. The effect of the grinding is also remarkable: the LM sample shows

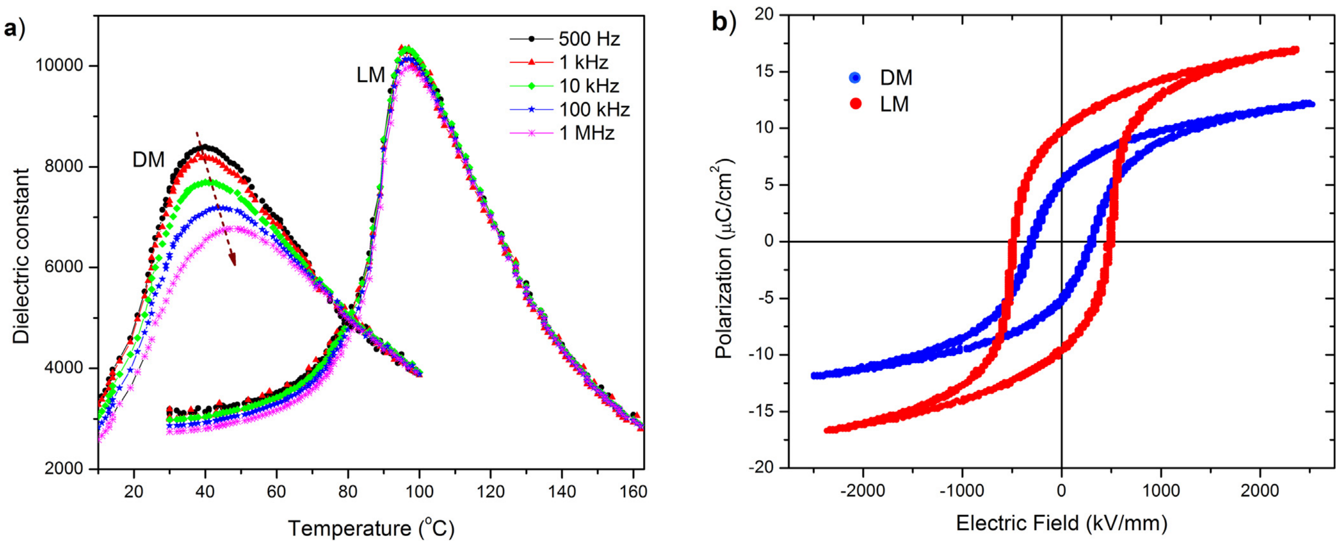

Fig. 3. (a) Temperature dependence of the dielectric constants of BCZT ceramics fabricated with powders milled in liquid medium (LM), and milled in dry conditions (DM). The data were taken during the heating process of the thermal cycle. (b) Polarization hysteresis loops of the ceramics measured at 50 Hz.

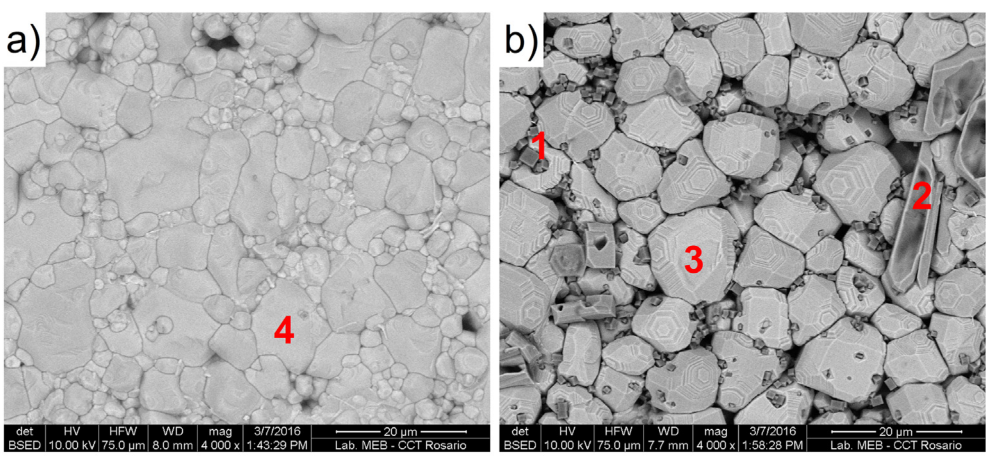

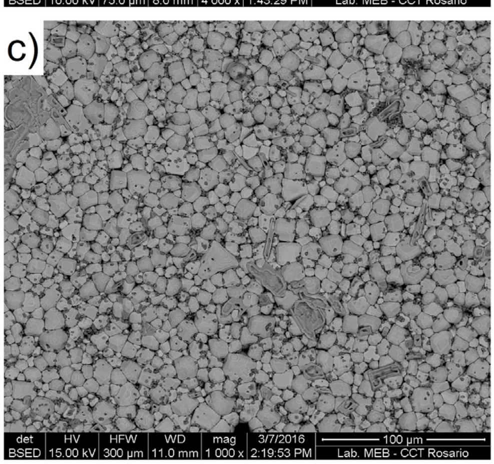

d)

Zone → / Elements ↓	1	2	3	4
Ca	13.0	1.4	2.7	2.8
Ba	3.3	8.9	15.3	15.0
Zr	0.8	0.7	3.4	2.1
Ti	22.9	24.0	19.2	19.5
O	60.0	65.0	59.4	60.6

Fig. 4. SEM images showing surface morphologies of BCZT ceramics sintered with powders milled in liquid medium (a), and milled in dry conditions (b and c). (d) EDX analysis for the regions identified in (a) and (b).

a well-developed and broad ferroelectric loop while the DM ceramic presents a smaller loop. The remnant polarization is about half of the LM one. Regarding the piezoelectric response, the d_{33} coefficient measured for the LM ceramic (380 pC/N) is significantly higher than that of the DM sample (90 pC/N).

SEM of the surface samples shows that while the LM ceramic displays a dense microstructure with a bimodal grain size distribution (Fig. 4a), the DM sample shows structural inhomogeneity (Fig. 4b). Three different regions can be distinguished: (1) grains similar to the ones observed in the LM sample, (2) small dark cubes, and (3) regions of irregular shape. The low magnification image of Fig. 4c shows that these inhomogeneities are distributed throughout the surface of the sample. We present in Fig. 4d the results of EDX analysis of the regions. The elementary composition analysis and the X-ray pattern shown in Fig. 2b allow us to conclude that BCZT grains, amorphous regions rich in Ba and Ti, and $CaTiO_3$ nanocubes coexist in the DM sample. It is interesting to note that the two additional phases have low zirconium content and, therefore, the remaining BCZT phase turns out to be rich in Zr. This explains the shift to lower temperatures and the relaxor behavior reported in Fig. 3a. The high Zr content also explains the worsening of ferroelectric and piezoelectric properties [14].

In summary, the electrical properties of BCZT ceramics depend strongly on the grinding intensity of the calcined powders. We have checked that the reported features also hold for ceramics sintered for longer dwell time (12 h) or at higher temperature (1500 °C). It was also verified that the effects produced by the dry milling cannot be attributed to the wearing of the ZrO_2 balls. Finally, we note that the condition of dry milling used in this work should be considered as an extreme case, chosen to maximize the grinding effects on material properties. Given that the intensity of grinding depends on the powder/liquid ratio, this ratio should be as low as possible. If this is not accomplished, the secondary phases observed in this study could be present but to a lesser extent, even without being detected in X-ray patterns.

4. Conclusions

We show that the grinding intensity of calcined BCZT powders is a key parameter for proper sintering of ceramics. A high energy milling deteriorates the piezoelectric response due to the development of an inhomogeneous microstructure, which is originated from a mechanically induced phase decomposition process. The resulting microstructure consists of BCZT grains rich in Zr, $CaTiO_3$ nanocubes and an amorphous phase rich in Ba and Ti. Post-calcination grinding is a necessary step to manufacture dense ceramics, since sintering necks can generate pores. In BCZT, the milling must be performed in abundant liquid medium to prevent the activation of unwanted phases.

Acknowledgments

This work was sponsored by CONICET and ANPCyT de la República Argentina. MGS thanks support from CIUNR.

References

[1] M. Maerder, D. Damjanovic, N. Setter, Lead free piezoelectric materials, J. Electroceram. 13 (2004) 385–392.
[2] P. Panda, Review: environmental friendly lead-free piezoelectric materials, J. Mater. Sci. 44 (2009) 5049–5062.
[3] J. Rödel, W. Jo, K. Seifert, E. Anton, T. Granzow, D. Damjanovic, Perspective on the development of lead-free piezoceramics, J. Am. Ceram. Soc. 92 (2009) 1153–1177.
[4] S. Leontsev, R. Eitel, Progress in engineering high strain lead-free piezoelectric ceramics, Sci. Technol. Adv. Mater. 11 (2010) 044302.
[5] D. Xiao, Progresses and further considerations on the research of perovskite lead-free piezoelectric ceramics, J. Adv. Dielect. 1 (2011) 33–40.
[6] J. Rödel, K. Webber, R. Dittmer, W. Jo, M. Kimura, D. Damjanovic, Transferring lead-free piezoelectric ceramics into application, J. Eur. Ceram. Soc. 35 (2015) 1659–1681.
[7] W. Liu, X. Ren, Large piezoelectric effect in Pb-free ceramics, Phys. Rev. Lett. 103 (2009) 257602.
[8] D. Keeble, F. Benabdallah, P. Thomas, M. Maglione, J. Kreisel, Revised structural phase diagram of $(Ba_{0.7}Ca_{0.3}TiO_3)$-$(BaZr_{0.2}Ti_{0.8}O_3)$, Appl. Phys. Lett. 102 (2013) 092903.
[9] J. Hao, W. Bai, W. Li, J. Zhai, Correlation between the microstructure and electrical properties in high-performance $(Ba_{0.85}Ca_{0.15})(Zr_{0.1}Ti_{0.9})O_3$ lead-free piezoelectric ceramics, J. Am. Ceram. Soc. 95 (2012) 1998–2006.
[10] Y. Tian, X. Chao, L. Wei, P. Liang, Z. Yang, Phase transition behavior and electrical properties of lead-free $(Ba_{1-x}Ca_x)(Zr_{0.1}Ti_{0.9})O_3$ piezoelectric ceramics, J. Appl. Phys. 113 (2013) 184107.
[11] W. Li, Z. Xu, R. Chu, P. Fu, G. Zang, Polymorphic phase transition and piezoelectric properties of $(Ba_{1-x}Ca_x)(Ti_{0.9}Zr_{0.1})$O3 lead-free ceramics, Phys. B 405 (2010) 4513–4516.
[12] M. Jiang, Q. Lin, D. Lin, Q. Zheng, X. Fan, X. Hailing Sun, Y. Wan, L. Wu, Effects of MnO_2 and sintering temperature on microstructure, ferroelectric, and piezoelectric properties of $Ba_{0.85}Ca_{0.15}Ti_{0.90}Zr_{0.10}O_3$ lead-free ceramics, J Mater. Sci. 48 (2013) 1035–1041.
[13] P. Mishra, S. Sharma, P. Kumar, Effect of sintering temperature on dielectric, Piezoelectric and ferroelectric properties of BZT-BCT 50/50 ceramics, J. Alloys Compd. 545 (2012) 210–215.
[14] J. Wu, D. Xiao, W. Wu, Q. Chen, J. Zhu, Z. Yang, J. Wang, Composition and poling condition-induced electrical behavior of $(Ba_{0.85}Ca_{0.15})(Ti_{1-x}Zr_x)O_3$ lead-free piezoelectric ceramics, J. Eur. Ceram. Soc. 32 (2012) 891–898.